EUROPEAN ORGANIZATION FOR NUCLEAR RESEARCH

CERN-EP/79-159
19 December 1979

COHERENT A_2^- PRODUCTION ON NUCLEI OBSERVED IN THE $K^-K_S^0$ DECAY CHANNEL AT 17.2 GeV/c

(CERN-Munich Collaboration)

V. Chabaud, B. Hyams, T. Papadopoulou*), K. Rybicki**) and P. Weilhammer

CERN, Geneva, Switzerland

H. Becker***), G. Blanar, M. Cerrada†), H. Dietl, J. Gallivan††),
B. Gottschalk†††), E. Lorenz, G. Lütjens, G. Lutz, W. Männer,
B. Niczyporuk**), D. Notz×), R. Richter, U. Stierlin,
B. Stringfellow××) and M. Turala**)

Max Planck Institute, Munich, Germany

J. De Groot†)

Zeeman Laboratory, Amsterdam, The Netherlands

ABSTRACT

We have studied A_2^- production by π^- on a nuclear target in the $K^-K_S^0$ decay channel, where the A_2^- is observed above a small background at 17.2 GeV/c incident momentum. Direct confirmation of coherent A_2 ($J^P = 2^+$) production has been found.

(Submitted to Physics Letters B)

*) Now at the National Technical University, Athens, Greece.
**) On leave of absence from the Institute of Nuclear Physics, Cracow, Poland.
***) Now at Technische Fachhochschule, Saarbrücken, Germany.
†) Now at CERN, Geneva, Switzerland.
††) Now at British National Oil Corporation, Glasgow, United Kingdom.
†††) Now at Northeastern University, Boston, Mass., USA.
×) Now at DESY, Hamburg, Germany.
××) Now at the Nuclear Research Centre, Strasbourg, France.

1. INTRODUCTION

The coherent production on nuclear targets has been observed to follow the so-called "Gribov-Morrison" empirical rule [1]. Thus for incoming pions or kaons the unnatural spin-parity states with $J^P = 0^-, 1^+, 2^-$ are coherently produced (see, for example, Pernegr et al. [2]). An exception to this rule has been observed for the A_2^- ($J^P = 2^+$) coherent production in Pernegr et al. [2] and Kruse et al. [3]. In these papers, an extraction of the A_2^- signal from a large background required a model-dependent partial wave analysis of the $\pi^+\pi^-\pi^-$ state. Since the coherent process (interaction with many nucleons inside the nucleus) is dominated by diffractive dissociation, this may mean that the A_2 production mechanism has a strong diffractive component. This is independently confirmed by the well-known weak energy dependence of the A_2 production off hydrogen (see, for example, Chabaud et al. [4], Daum et al. [5], and Hyams et al. [6]).

In this work we study the A_2 production on a polarized butanol (C_4H_9OH) target measuring the reaction

$$\pi^- \text{ nucleus} \rightarrow K^-K_S^0 \text{ nucleus}, \quad K_S^0 \rightarrow \pi^+\pi^- .$$

In the analysis we do not make use of the polarization of the hydrogen in the target, but rather investigate the properties of A_2 production on the carbon and oxygen nuclei. An advantage of the $K^-K_S^0$ decay channel is an observation of A_2 over a small background.

2. EXPERIMENTAL APPARATUS

The experiment was performed with the CERN-Munich (MPI) spectrometer at the CERN Proton Synchrotron (PS) (Fig. 1). It is described in detail in De Groot [7] and Becker et al. [8].

The particle trajectories are measured by magnetostrictive spark chambers (SCh). The beam particles are momentum analysed by a beam spectrometer M and identified by a beam Čerenkov counter $\check{C}_1$. The target T suspended inside a 25 kG homogeneous magnetic field is surrounded by a veto box of tungsten-scintillator shower counters F which veto events with π^0's and charged recoil particle multiplicities above one. A 36-element hodoscope of overlapping scintillation counters measured the azimuthal angle of the recoil proton, thus allowing for $|t| > 0.08$ GeV/c^2 an off-line determination of the coplanarity of the reaction. Multiwire proportional chambers (MWPC) in front of and behind the target improved the accuracy of vertex determination in the magnetic field. The pulse height in a 1 mm thick scintillation counter K directly behind the target allowed the determination of the charged particle multiplicity. The counters V and H in front of and inside the spectrometer magnet (AEG) vetoed events with additional particles missing the spectrometer aperture. A double-layer scintillator hodoscope EG measured the charged particle multiplicity of particles traversing the spectrometer. The multicell Čerenkov counters $\check{C}_2$ and $\check{C}_3$ were not used in this analysis.

The trigger for the reaction (1) was: a beam pion defined by signals from the scintillation counters $B_1 \cdot B_2 \cdot B_3 \cdot \overline{B_4}$ and the Čerenkov $\check{C}_1$, a hit from one charged particle in the K-counter, three hits in the EG array, an interaction signalled by a hit in a scintillation counter I -- which has a hole at the position of the beam --, zero or one signal in veto counters F and no hit in the veto counter D. About 500,000 such triggers were collected.

3. DATA ANALYSIS

In a geometry reconstruction program events were selected using the following criteria: i) three secondaries of total charge -1; ii) one of the negative secondaries forms a vertex with the beam track inside the target; iii) the other two tracks come from a second vertex downstream of the K-counter. The invariant mass $m_{\pi^+\pi^-}$ of the latter two particles showed a prominent K^0_S peak. Events were selected around the K^0_S peak in the mass interval $0.486 < m_{\pi^+\pi^-} < 0.510$ GeV. Interpreting the negative track not associated with the K^0_S as a K^-, an appropriate cut in the missing mass recoiling to the $K^-K^0_S$ system is applied, essentially requiring the target nucleus to have the same mass after the interaction. This procedure leaves approximately 5000 events in the mass region $1.21 \leq m_{K^0_S K^-} \leq 1.41$ GeV.

The intensity and angular distribution were calculated using a maximum likelihood method to correct for the limited geometrical acceptance of our apparatus as described in Chabaud et al. [4].

4. RESULTS AND DISCUSSION

The distribution of $K^-K^0_S$ acceptance-corrected invariant mass is plotted in Fig. 2. It is parametrized by a spin-2 Breit-Wigner form on an incoherent linear background contribution. The fit gives a mass = 1320 ± 2 MeV and a width $\Gamma = 106 \pm 4$ MeV with a $\chi^2/NDF = 4.6/7$ in agreement with the resonance parameters compiled by the Particle Data Group [9].

We note the small background contribution which is 14% of the total number of events in the $1.21 \leq m_{K^-K^0_S} \leq 1.41$ GeV region.

The distribution of $t' = |t - t_{min}|$ for all events in the A_2 mass interval 1.21-1.41 GeV (Fig. 3a) exhibits the coherent A_2 production on carbon. It has a dip in the forward direction characteristic of helicity flip $|\Delta M| = 1$ production; it then increases with t' and after reaching a maximum falls off with the nuclear form factor as $e^{-\alpha t'}$. Above $t = 0.1$ GeV^2 the incoherent part takes over. We have fitted the data with a two-term form

$$\frac{d\sigma}{dt'} = a\, t'\, e^{-\alpha t'} + b\, t'\, e^{-\beta t'} ,$$

where the exponent α of coherent production is $\alpha = (43 \pm 2)$ (GeV/c)$^{-2}$ and the exponent of incoherent production is $\beta = (8 \pm 1)$ (GeV/c)$^{-2}$, with $\chi^2/NDF = 16.5/15$. The first term accounts for (30 ± 1)% of the cross-section integrated over t'.

The exponents of the coherent (α) and incoherent (β) part of the t' distribution are compatible with the naive expectation for coherent production $\alpha = \beta A^{2/3}$ and the measurements of the $A_2^\pm$ production on hydrogen [4,8], respectively.

For $t' \geq 0.08$ GeV we are able to separate, in our sample, events produced off hydrogen from those produced off carbon and oxygen atoms in the butanol target. This is done by requiring coplanarity between the $K^-K^0_S$ system and the recoil proton as measured with the coplanarity hodoscope around the target (Fig. 4). For a cut in the coplanarity angle $\Delta\phi$ of ±10° we estimate a background of (48 ± 7)% from events not coming from free hydrogen.

This background contains events on bound protons, genuine inelastic events, and a very small flat contribution caused by delta-rays accidentally hitting the coplanar hodoscope elements. It is indicated by a dashed line in Fig. 4.

The t' distribution for events with the $\pm 10°$ $\Delta\phi$ cut is shown in Fig. 3b; a fit with $b' e^{-\beta' t'}$ yields $\beta' = (7.8 \pm 0.2)$ $(\text{GeV}/c)^{-2}$, $\chi^2/\text{NDF} = 2/8$, in agreement with the incoherent part of the previous distribution.

The simultaneous measurement of A_2 production on hydrogen and on butanol allows us to estimate the cross-section on butanol from earlier measurements of the hydrogen cross-section [8] and the butanol/hydrogen event ratio as observed in this experiment. We obtain $\sigma_B = (122 \pm 30)$ μb for the A_2^- production on butanol (C_4H_9OH) with a subsequent decay into a $K^-K^0_S$ channel. Further, assuming that the cross-section on the single oxygen nucleus in the butanol molecule has the value of $16/12$ times the carbon cross-section, we calculate the following values of the coherent and incoherent A_2^- production cross-section on carbon

$$\left.\begin{array}{l} \sigma_c^{coh} = (6.9 \pm 1.7)\ \mu b \\ \sigma_c^{inc} = (13.5 \pm 7.5)\ \mu b \end{array}\right\} \quad \text{for the decay channel } A_2 \to K^-K^0, \quad K^0 \to \pi^+\pi^- .$$

These values refer to the mass range between 1.2 GeV and 1.42 GeV and to the t' below 0.8 GeV^2/c^2. Comparing the coherent cross-section σ_c^{coh} with the value $\sigma_H = 1.1$ mb [4] obtained for the same reaction on a hydrogen target, we see again the ratio of ~ 6 compatible with the naive expectation of $A^{2/3}$ for the coherent production on carbon.

Correcting for the unobserved decay channels ($A_2 \to K^-K^0_L$, $K^0_S \to \pi^0\pi^0$) and taking the branching ratio of $(4.7 \pm 0.5)\%$ for $A_2 \to \bar{K}K$ from ref. [9], we obtain a considerable cross-section of (440 ± 120) μb for the A_2 coherent production on carbon. Let us remember that the cross-section for the A_1 coherent production on carbon is of the order of 1 mb [10].

The t-channel moments of the decay angular distribution $\langle Y^\ell_m \rangle = \int (d\sigma/d\Omega) Y^\ell_m(\Omega)\, d\Omega$ were determined as a function of t' averaged over the whole A_2 mass interval $1.21 < m_{K^-K^0_S} < 1.41$ GeV (Fig. 5). Y^ℓ_m are the spherical harmonics, $\Omega \equiv (\cos\theta, \phi)$

represents the decay angles of the K^- in the $K^-K^0_S$ rest system. In the fit to the data all moments up to $\ell = 4$ corresponding to angular momentum states $L = 2$ were allowed. All moments except $\langle Y^2_0 \rangle$, $\langle Y^2_2 \rangle$, $\langle Y^4_0 \rangle$, and $\langle Y^4_2 \rangle$ were compatible with zero and neglected in the final fit. No significant variation with momentum transfer t' is seen in the four non-zero moments, indicating that the mechanism responsible for coherent and incoherent A_2 production is of the same nature. The same moments measured in A_2^- production at 9.8 and 18.8 GeV [4] and in A_2^+ production at 12.7 GeV [6] on a hydrogen target are compatible with the values found here for $|t| \gtrsim 0.1$ GeV^2. This suggests the same production mechanism off nuclei and off hydrogen. A strong coherent production of A_2 indicates that this mechanism has a diffractive component.

5. CONCLUSIONS

A strong coherent A_2^- production by π^- on a nuclear target has been observed in the $A_2^- \rightarrow K^-K^0_S$ decay channel. The cross-section for coherent A_2 production on a carbon nucleus is estimated to be $\sigma_c^{coh} = (0.44 \pm 0.12)$ mb. The observed decay angular distribution as a function of t' suggests the same A_2 production mechanism off nuclei and off hydrogen.

Acknowledgements

Some of us wish to express their gratitude to CERN (K.R.) and others to the Max Planck Institute (J. De G. and T.P.) for support and hospitality during the experiment. One of us (T.P.) would like to thank Dr. E.J. Sacharidis for valuable discussions.

REFERENCES

[1] D.R.O. Morrison, Phys. Rev. 165 (1968) 1699.

[2] J. Pernegr et al., Nucl. Phys. B134 (1978) 436.

[3] U.E. Kruse et al., Phys. Rev. Lett. 32 (1974) 1328.

[4] V. Chabaud et al., Nucl. Phys. B145 (1978) 349.

[5] C. Daum et al., preprint CERN-EP/79-109, submitted to Phys. Lett. B.

[6] B. Hyams et al., Nucl. Phys. B146 (1978) 303.

[7] J.G.H. De Groot, Thesis, University of Amsterdam (April 1978).

[8] H. Becker et al., Nucl. Phys. B150 (1979) 301.

[9] Particle Data Group, Review of Particle Properties, Phys. Lett. 75B (1978).

[10] W. Beusch et al., Phys. Lett. 55B (1975) 98.

Figure captions

Fig. 1 : Schematic view of the apparatus. In the lower part, anticoincidence counters and the coplanarity hodoscope around the target are shown enlarged.

Fig. 2 : $K^-K^0_S$ mass spectrum. The solid line is obtained from a fit using a Breit-Wigner form on a linear background contribution which is represented by a dashed line.

Fig. 3 : Differential cross-sections for π^- nucleus $\to$ ($A_2 \to K^-K^0_S$) nucleus as a function of t':

a) for all the events in the mass interval 1.21 GeV $< m_{K\bar{K}} <$ 1.41 GeV;

b) for events in the same mass interval but with a coplanarity cut $|\Delta\phi| \leq 10°$.

The curves are the results of fits to the exponential forms.

Fig. 4 : The distribution of the coplanarity angle $\Delta\phi$. $\Delta\phi$ is the difference between the azimuth of the missing recoil momentum and the azimuth corresponding to the closest hit in the hodoscope around the target.

Fig. 5 : Normalized moments, $\langle Y^\ell_m \rangle$, as a function of t'. All moments are normalized such that $\langle Y^0_0 \rangle = 1/\sqrt{4\pi}$.

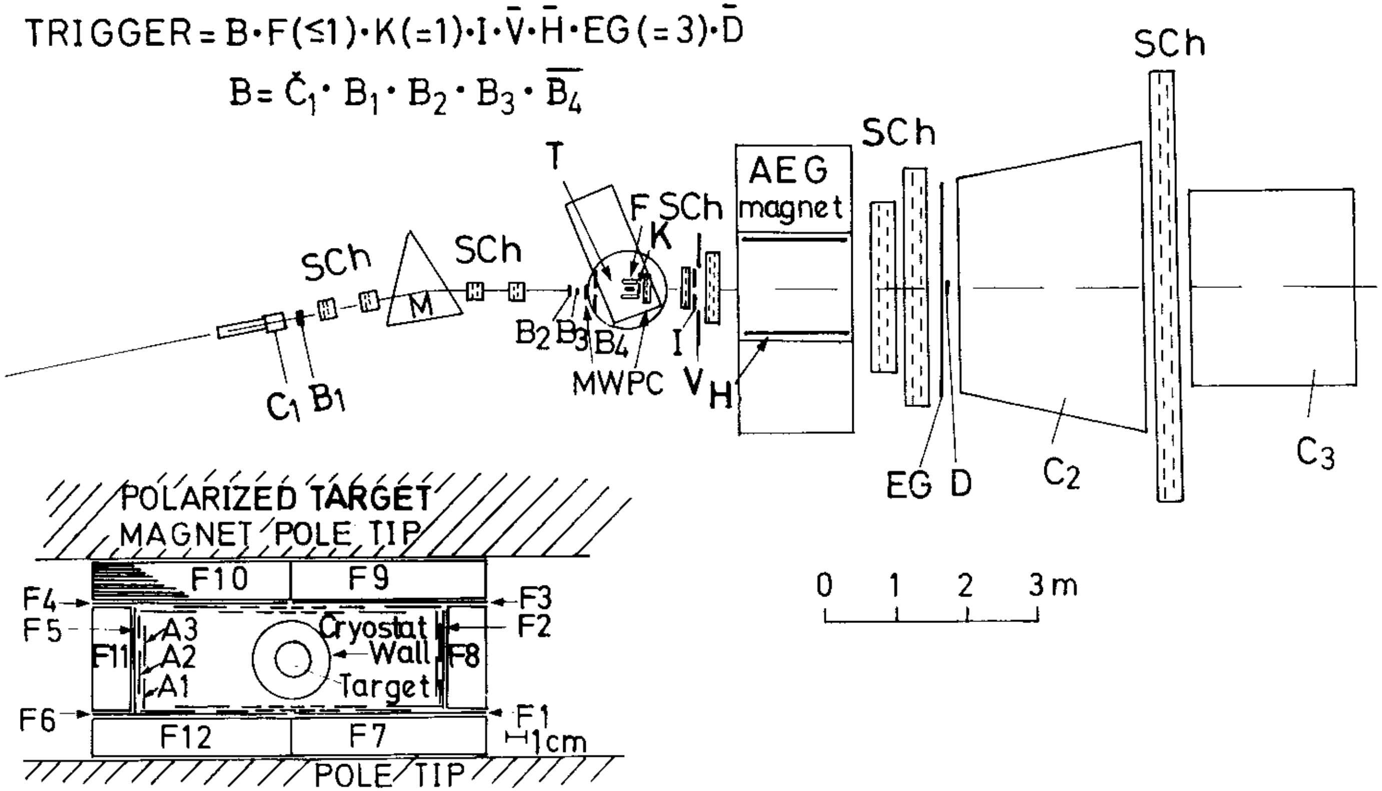
TRIGGER = B·F(≤1)·K(=1)·I·V̄·H̄·EG(=3)·D̄
B = Č1·B1·B2·B3·B̄4
SCh
SCh
SCh
SCh
SCh
M
T
F
K
B2
B3
B4
MWPC
I
V
H
C1
B1
AEG
magnet
EG
D
C2
C3
0 1 2 3m
POLARIZED TARGET
MAGNET POLE TIP
F10
F9
F4
F3
F5
F2
A3
A2
A1
F11
F8
Cryostat
Wall
Target
F6
F1
F12
F7
1cm
POLE TIP

Fig. 1

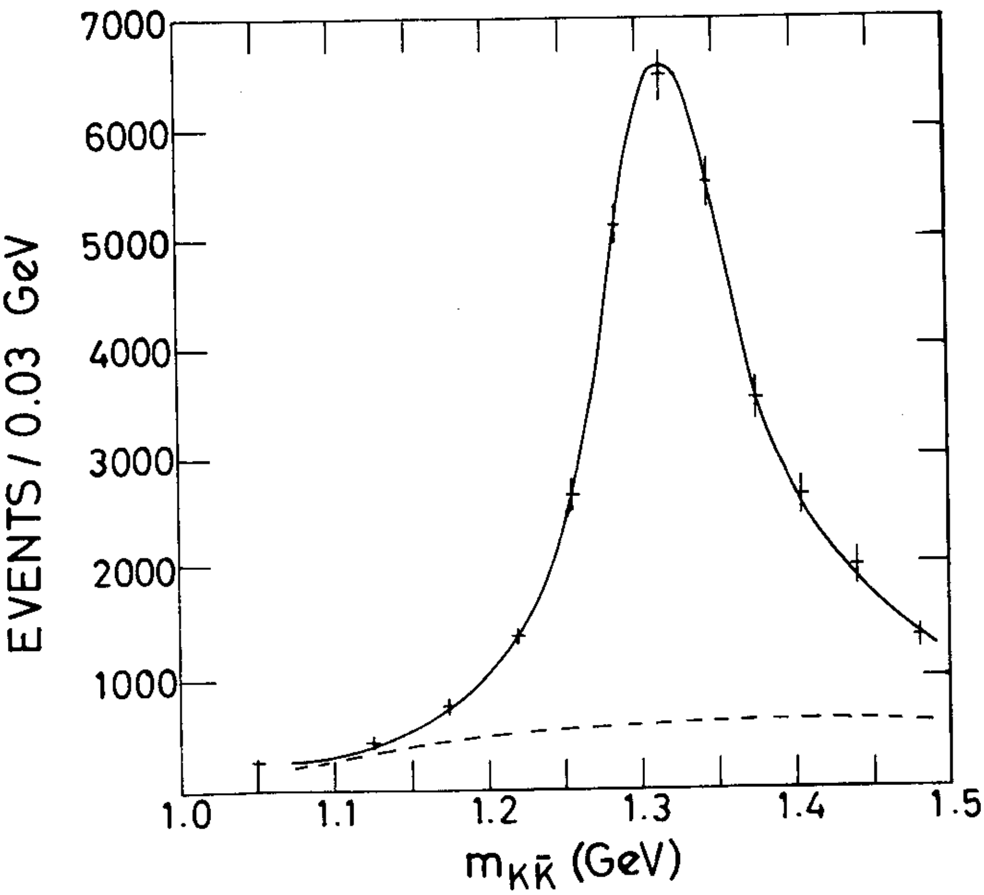

7000
6000
5000
4000
3000
2000
1000
EVENTS / 0.03 GeV
1.0
1.1
1.2
1.3
1.4
1.5
$m_{K\bar{K}}$ (GeV)

Fig. 2

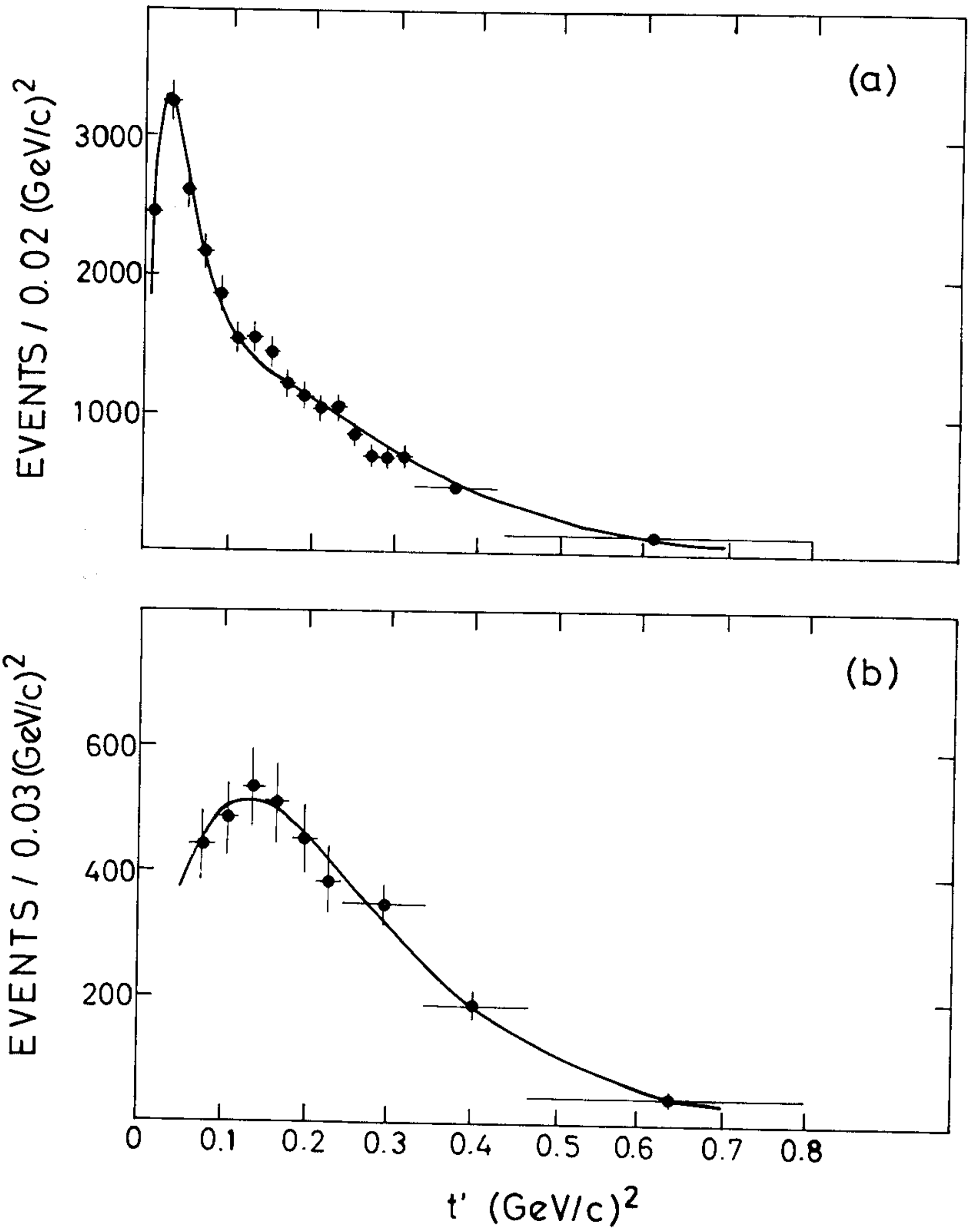

(a)
EVENTS / 0.02 (GeV/c)^2
3000
2000
1000
(b)
EVENTS / 0.03 (GeV/c)^2
600
400
200
0
0.1
0.2
0.3
0.4
0.5
0.6
0.7
0.8
t' (GeV/c)^2

Fig. 3

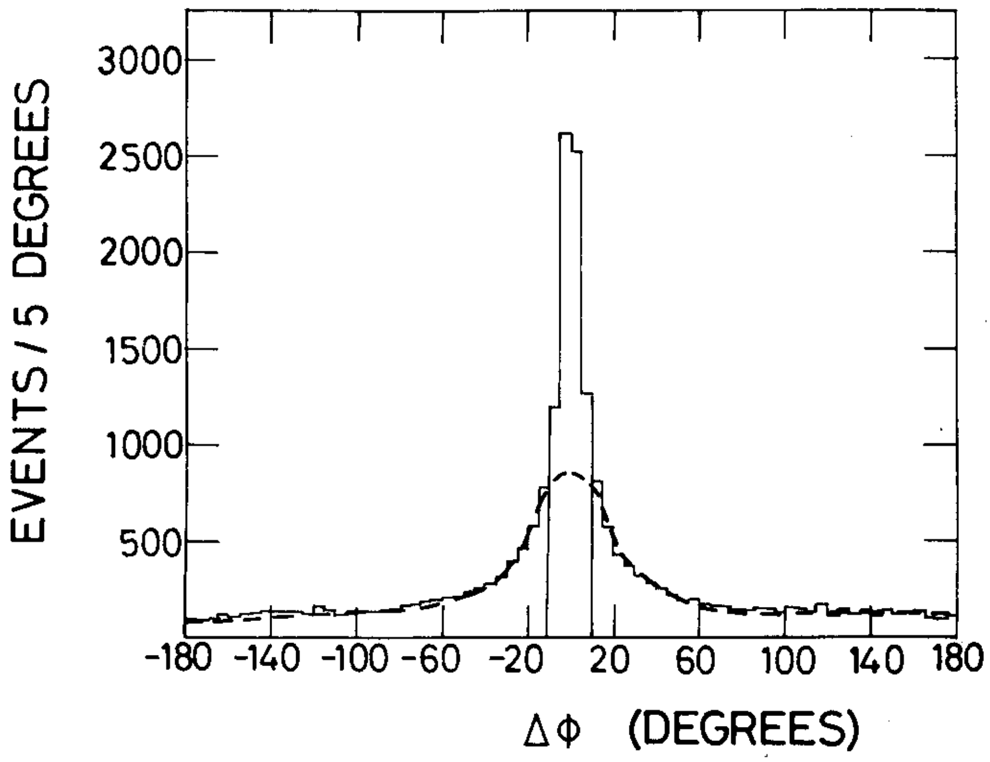

EVENTS / 5 DEGREES
3000
2500
2000
1500
1000
500
-180
-140
-100
-60
-20
20
60
100
140
180
ΔΦ (DEGREES)

Fig. 4

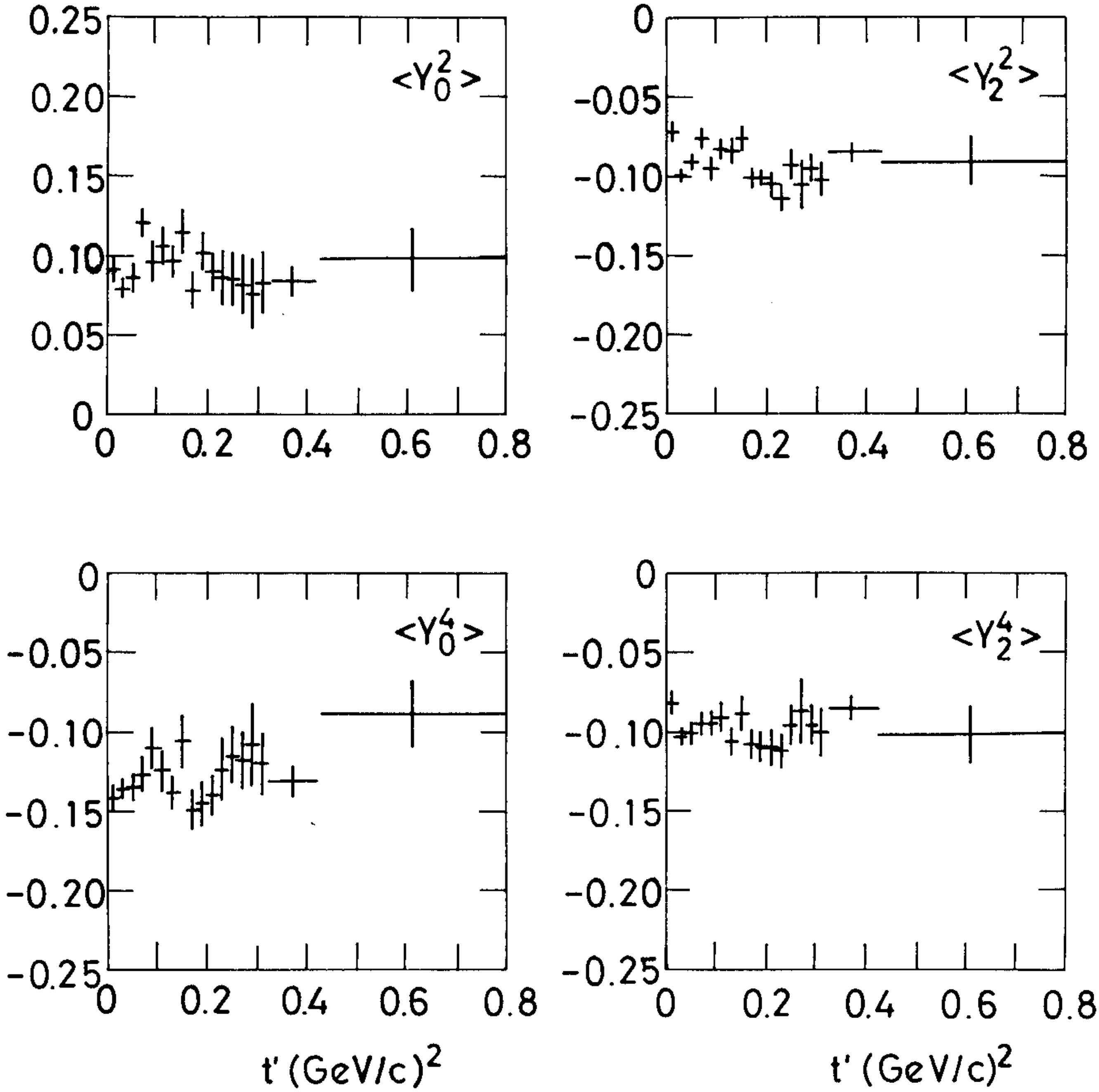

0.25
0.20
0.15
0.10
0.05
0
0.2
0.4
0.6
0.8
$<Y_0^2>$
-0.05
-0.10
-0.15
-0.20
-0.25
$<Y_2^2>$
$<Y_0^4>$
$<Y_2^4>$
t' (GeV/c)^2
t' (GeV/c)^2

Fig. 5